Pair annihilation reaction $D+D\rightarrow 0$ in disordered media and conformal invariance

F. C. Alcaraz*
Instituto de Física de São Carlos, Universidade de São Paulo, Caixa Postal 369, 13560-590 São Carlos, São Paulo, Brazil

V. Rittenberg†
Physikalisches Institut, Bonn University, 53115 Bonn, Germany
and Department of Mathematics and Statistics, University of Melbourne, Parkville, Victoria 3010, Australia

(Received 11 December 2006; revised manuscript received 27 March 2007; published 14 May 2007)

The raise and peel model is a stochastic model of a fluctuating interface separating a substrate covered with clusters of matter of different sizes and a rarefied gas of tiles. The stationary state is obtained when adsorption compensates the desorption of tiles. This model is generalized to an interface with defects (D). The defects are either adjacent or separated by a cluster. If a tile hits the end of a cluster with a defect nearby, the defect hops at the other end of the cluster, changing its shape. If a tile hits two adjacent defects, the defects annihilate and are replaced by a small cluster. There are no defects in the stationary state. This model can be seen as describing the reaction $D+D\rightarrow 0$, in which the particles (defects) D hop at long distances, changing the medium, and annihilate. Between the hops the medium also changes (tiles hit clusters, changing their shapes). Several properties of this model are presented and some exact results are obtained using the connection of our model with a conformally invariant quantum chain.

DOI: 10.1103/PhysRevE.75.051110 PACS number(s): 05.50.+q, 47.27.eb, 05.70.−a

I. INTRODUCTION

The raise and peel model [1,2], which is a stochastic model of a fluctuating interface, is, to our knowledge, the first example of a stochastic model that has the space-time symmetry of conformal invariance. This implies that the dynamic critical exponent $z=1$ and certain scaling properties of various correlation functions are known. This model was extended in order to take into account sources at the boundaries [3–5], keeping conformal invariance. In all these cases, the stationary states have magic combinatorial properties.

In the present paper we describe another extension of the raise and peel model keeping conformal invariance (see also Appendixes A and B) by introducing defects on the interface. These defects hop at long distances in a medium which is changed by the hops. Between the hops the medium also changes. Finally, when two defects touch, they can annihilate. The stationary state is the same one as in the original raise and peel model with no defects.

The whole process can be seen as a reaction $D+D\rightarrow 0$, where D is a defect, taking place in a disordered unquenched medium.

In Sec. II we describe the model. Like the raise and peel model [1], the present model comes from considering the action of a Hamiltonian expressed in terms of Temperley-Lieb generators on a vector space that is a left ideal of the Temperley-Lieb algebra. The ideal can be mapped on graphs that constitute the configuration space of the model. We briefly review in Appendix A the mathematical background of the model and refer for details to Refs. [4,5].

In Sec. III, using Monte Carlo simulations, we describe the long-range hopping of defects and give the Lévy flight probability distribution.

In Sec. IV, again using Monte Carlo simulations, starting with a configuration that consists only of defects, we study the variation in time t of their density for a lattice of size L. We obtain the scaling function that gives the number of defects in terms of t/L, and show how conformal invariance gives some of its properties. In the thermodynamic limit the density decreases in time as $1/t$, as is expected since in a conformally invariant theory time and space are on equal footing. In Sec. V we present our conclusions.

II. THE RAISE AND PEEL MODEL WITH DEFECTS

We consider an interface of a one-dimensional lattice with $L+1$ sites. An interface is formed by attaching at each site a non-negative integer height h_i $(i=0,1,\ldots,L)$. We take $h_0=h_L=0$. If for two consecutive sites j and $j+1$ we have $h_j=h_{j+1}=0$, on the link connecting the two sites we put an arrow called a defect (see Fig. 1). For the remaining sites, the heights obey the restrict solid-on-solid (RSOS) rules:

$$h_{i+1}-h_i=\pm 1, \quad h_i\geq 0. \tag{1}$$

A domain in which the RSOS rules are obeyed $\{h_j=h_l=0, h_k>0, j<k<l\}$ is called a cluster. There are three clusters and three defects in Fig. 1 $(L=21)$. There are $\binom{L}{[L/2]}$

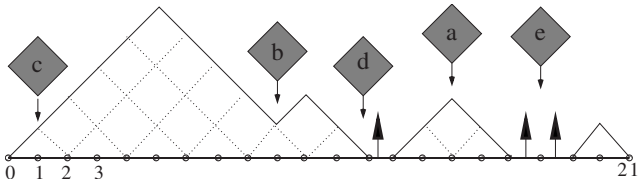

FIG. 1. One of the configurations for $L=21$ (22 sites). There are three defects (arrows on the links) and three clusters. Also shown are five tiles (tilted squares) a–e belonging to the gas. When a tile hits the surface, the effect is different in the five cases.

*Electronic address: alcaraz@if.sc.usp.br
†Electronic address: vladimir@th.physik.uni-bonn.de

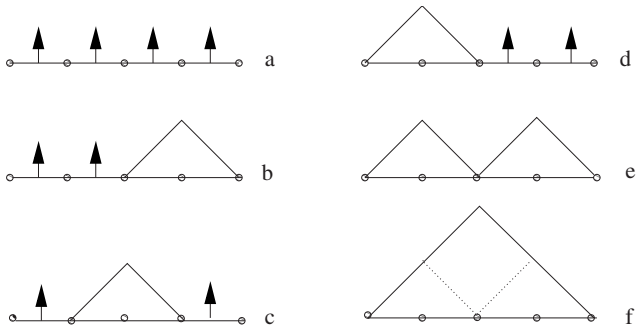

FIG. 2. The six configurations for $L=4$ (five sites). In the stationary state only the RSOS configurations (e) and (f) occur.

possible configurations of the interface (we denote by $[x]$ the integer part of x).

There is a simple bijection between the configurations of interfaces and defects, where Fig. 1 is an example, and ballot paths [4]. A ballot path is obtained if one follows the RSOS rules (1), takes $h_L=0$, but leaves h_0 free $(0\leq h_L\leq L)$. This fact was used in [5] to define another stochastic model than the one described below. In the case $L=4$, the six possible configurations are shown in Fig. 2. The configuration shown in Fig. 2(b) has two defects and one cluster, while there are no defects in Fig. 2(f).

We consider the interface separating a film of tiles (clusters with defects) from a gas of tiles (tilted squares). The evolution of the system (Monte Carlo steps) is given by the following rules. With a probability $P_i=1/(L-1)$ a tile from the gas hits site i $(i=1,\ldots,L-1)$. As a result of this hit, the following effects can take place.

(a) The tile hits a local maximum of a cluster (a in Fig. 1). The tile is reflected.

(b) The tile hits a local minimum of a cluster (b in Fig. 1). The tile is adsorbed.

(c) The tile hits a cluster and the slope is positive $(h_{i+1}>h_i>h_{i-1})$ (c in Fig. 1). The tile is reflected after triggering the desorption of a layer of tiles from the segment $(h_j>h_i=h_{i+b},\ j=i+1,\ldots,i+b-1)$, i.e., $h_j\rightarrow h_j-2,\ j=i+1,\ldots,i+b-1$. The layer contains $b-1$ tiles (this is an odd number). Similarly, if the slope is negative $(h_{i+1}<h_i<h_{i-1})$, the tile is reflected after triggering the desorption of a layer of tiles belonging to the segment $(h_j>h_i=h_{i-b},\ j+i-b+1,\ldots,i-1)$.

(d) The tile hits the right end of a cluster $h_j>h(i-c)=h(i)=0$ $(j=i-c+1,\ldots,i-1)$ and $h(i+1)=0$. The link $(i,i+1)$ contains a defect (d in Fig. 1). The defect hops on the link $(c,c+1)$ after triggering the desorption of a layer of tiles $(h_j\rightarrow h_j-2,\ j=i-c+1,\ldots,i-1)$ and the tile is adsorbed, producing a new small cluster $(h_{i-1}=h_{i+1}=0,\ h_i=1)$ (see Fig. 3). If the defect is at the left end of a cluster, the rules are similar, the defect hops to the right after peeling the cluster, and a new small cluster appears at the end of the old one.

(e) The tile hits a site between two defects $(h_{i-1}=h_i=h_{i+1}=0)$. This is the case e in Fig. 1. The two defects annihilate and in their place appears a small cluster $(h_{i-1}=h_{i+1}=0,\ h_i=1)$. See Fig. 4.

To sum up, the defects (D) hop nonlocally in a disordered (not quenched) medium, which changes between successive

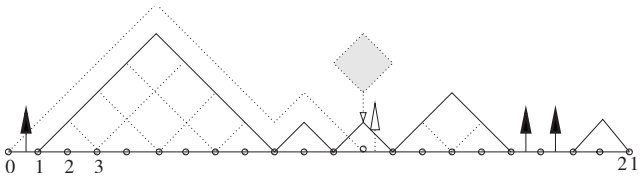

FIG. 3. The new profile after the tile d in Fig. 1 has hit the surface at the right end of a cluster. The defect hops to the left end of the cluster, peeling one layer, and a new small cluster appears at the right of the old cluster.

hops (local adsorption and nonlocal desorption take place in the clusters). During the hop, the defect peels the cluster and therefore also changes the medium. The annihilation reaction $D+D\rightarrow 0$ is local. If one starts the stochastic process with a certain configuration [for example, only defects as in Fig. 3(a)], due to the annihilation process, for L even all the defects disappear and in the stationary state one has only clusters (RSOS configurations). The properties of the stationary states have been studied elsewhere [1,2]. In the case L odd, in the stationary states one has one defect. In the next section we are going to see how this defect hops and will observe that the defect behaves like a random walker performing Lévy flights. This will help us understand the annihilation process $D+D\rightarrow 0$ described in Sec. IV. The rules described above were obtained by using a representation of the Temperley-Lieb algebra in a certain ideal [3–5] (see Appendix A). The finite-size scaling of the Hamiltonian eigenspectrum is known from conformal field theory (see Appendix B); therefore the physical properties of the model can be traced back to conformal invariance.

III. THE RANDOM WALK OF A DEFECT

Before discussing the annihilation reaction of defects, it is useful to understand how defects hop. The simplest way to study the behavior of defects is to take the stationary states in the case L odd when we have only a single defect. Although there is a lot of information about these stationary states coming from combinatorics [5,6] and Monte Carlo simulations [5], the results we present here are additional.

One asks what is the probability $P(s)$ for a defect to hop, in one Monte Carlo step, for a distance s (we assume L very large). We first see if, on physical grounds, one cannot guess the result. Let us assume that the defect behaves like a ramdon walker and that $P(s)$ describes Lévy flights [7–10]. This implies that for large values of s we have

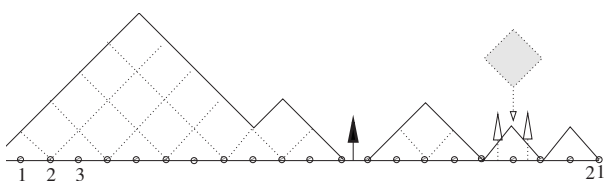

FIG. 4. The new profile after the tile e has hit the surface between two defects. The defects have disappeared and in their place one gets a new small cluster.

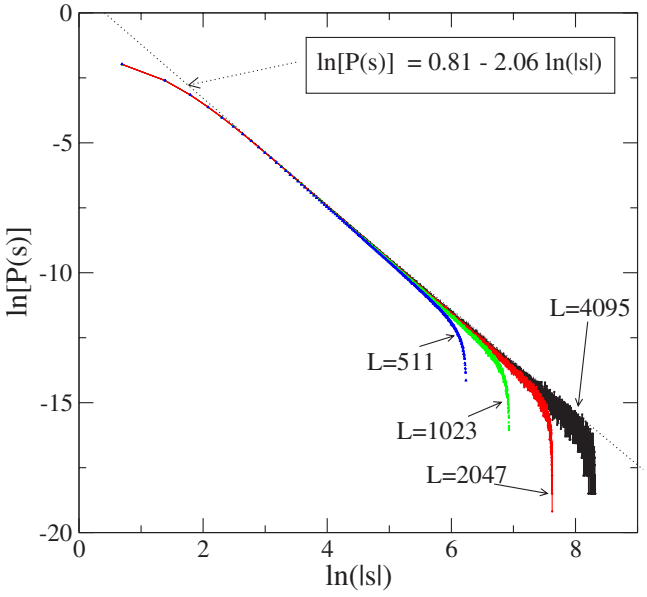

FIG. 5. (Color online) Probability $P(s)$ for a defect to hop a distance s in units of the lattice spacing. Monte Carlo simulations were done on systems of different sizes.

$$P(s) \sim \frac{1}{|s|^{1+\sigma}}. \tag{2}$$

If the random walker starts at a point $x=0$ (for example, in the middle of the lattice), at large values of t, the dispersion is [10]

$$\langle x^2 \rangle \sim t^{2/\sigma}. \tag{3}$$

In a conformally invariant model, one has no other scales but the size of the system; space and time are on equal footing and therefore one has to have $\sigma=1$.

In Fig. 5 we show $P(s)$ as obtained from Monte Carlo simulations for systems of different sizes. One notices a data collapse for a large domain of s. A fit to the data for the largest lattice ($L=4095$) gives, for large s,

$$P(s) \approx \frac{2.25}{|s|^{2.06}}, \tag{4}$$

in agreement with what we expected.

IV. THE DENSITY OF DEFECTS AT LARGE TIMES

We are now going to study the number of defects $N_d(t,L)$ as a function of time and lattice size, taking at $t=0$ the configuration where the lattice is covered by defects only [as in Fig. 2(a)]. An interesting aspect of this study is the role of conformal invariance. Since there are no other scales in the system except L, we expect for large values of t and L

$$N_d(t,L) = f\left(\frac{t}{L}\right). \tag{5}$$

In Fig. 6, we show $N_d(t,L)$ for various lattice sizes (L odd). One sees a nice data collapse except for very small values of t/L where the convergence is slower. A similar (but not identical) function is obtained for L even.

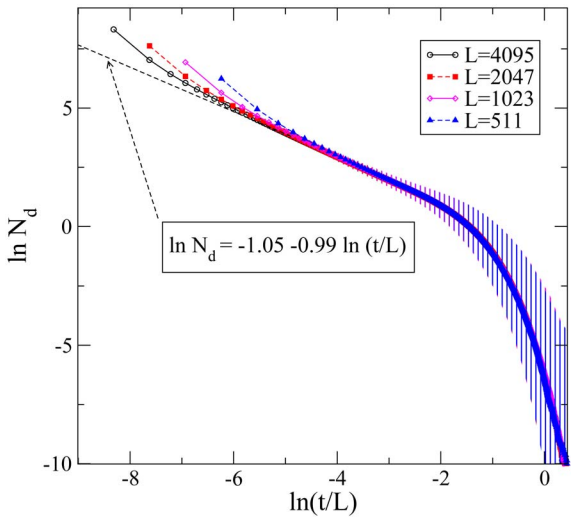

FIG. 6. (Color online) Number of defects $N_d(t,L)$ as a function of t/L for several lattice sizes (L odd). At $t=0$, $N_d(t=0,L)=L$. The error bars are also shown. The fitted linear curve shows that the density decreases as the inverse of time.

We first discuss the behavior of N_d for large values of t/L (see Fig. 7). A fit to the data gives (L odd)

$$N_d\left(\frac{t}{L}\right) = A_1^{(o)} e^{-\lambda_1^{(o)} t/L} + A_2^{(o)} e^{-\lambda_2^{(o)} t/L} + \cdots, \tag{6}$$

where

$$A_1^{(o)} = 6.75, \quad A_2^{(o)} = 17.27,$$

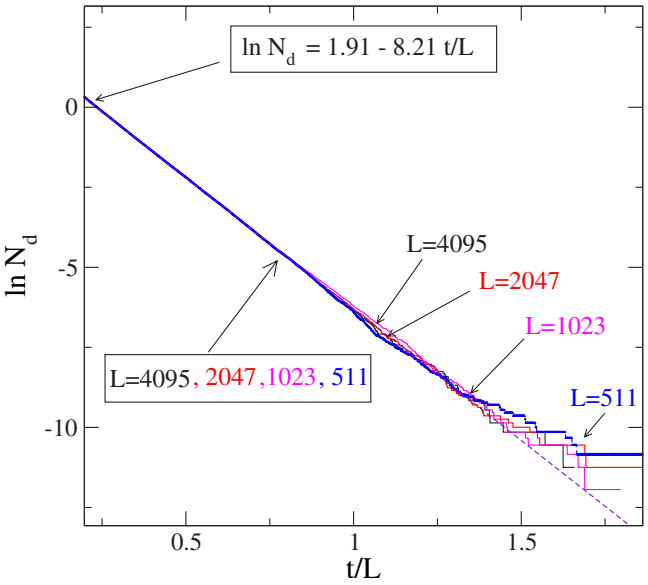

FIG. 7. (Color online) Number of defects N_d as a function of t/L as in Fig. 6 zoomed on the large time domain. The error bars, given in Fig. 6, are not shown.

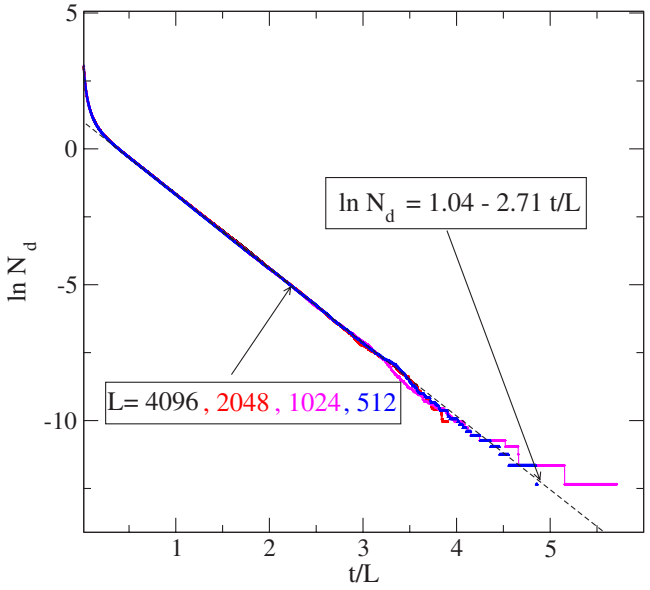

FIG. 8. (Color online) N_d as a function of t/L for large times for different lattice sizes (L even). The error bars are of the same order as in Fig. 6.

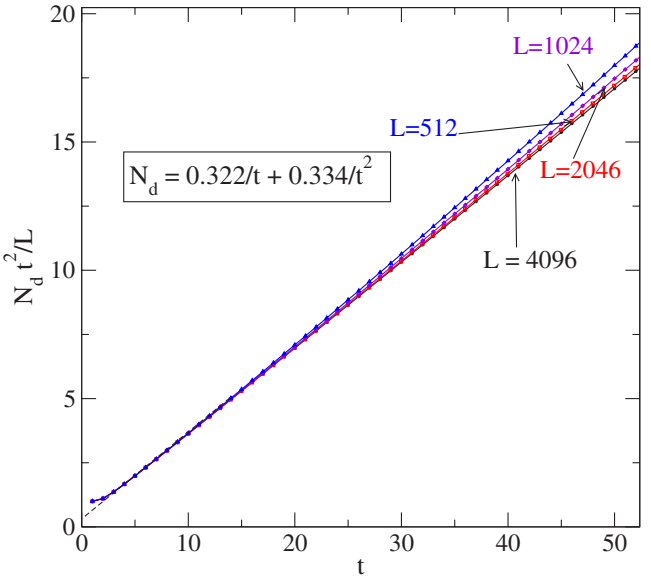

FIG. 9. (Color online) Density of defects times t^2 for short times. A linear fit to the data obtained for the largest lattice ($L=4096$) gives (14).

$$\lambda_1^{(o)} = 8.21, \quad \lambda_2^{(o)} = 26.48. \tag{7}$$

We can now compare the data obtained from the fit with the finite-size scaling spectrum of the Hamiltonian [see Appendix B, Eqs. (B8) and (B9)]:

$$\lambda_1^{(o)} = \frac{3\pi\sqrt{3}}{2} = 8.162\,097\,1\ldots,$$

$$\lambda_2^{(o)} = \frac{3\pi\sqrt{3}}{2}\frac{10}{3} = 27.206\,99\ldots. \tag{8}$$

No prediction can be made about $A_1^{(o)}$ or $A_2^{(o)}$ since they are not universal; they depend on the initial conditions. Notice that $A_2^{(o)} > A_1^{(o)}$, as it should be, since the expansion should diverge for short times where we expect

$$N_d \sim \frac{L}{t}. \tag{9}$$

A similar fit, done for L even (the data are shown in Fig. 8), gives

$$N_d\left(\frac{t}{L}\right) = A_1^{(e)} e^{-\lambda_1^{(e)} t/L} + A_2^{(e)} e^{-\lambda_2^{(e)} t/L} + \cdots, \tag{10}$$

with

$$A_1^{(e)} = 2.83, \quad A_2^{(e)} = 6.93,$$

$$\lambda_1^{(e)} = 2.71, \quad \lambda_2^{(e)} = 16.64. \tag{11}$$

We can again use the predictions of conformal invariance [see (B8) and (B9)] and get

$$\lambda_1^{(e)} = \frac{3\pi\sqrt{3}}{2}\frac{1}{3} = 2.720\,69\ldots,$$

$$\lambda_2^{(e)} = \frac{3\pi\sqrt{3}}{2}2 = 16.324\,194\ldots \tag{12}$$

to be compared with (11).

In the small t/L domain we get for L even and odd

$$\rho = \frac{N_d}{L} \approx \frac{0.322}{t}. \tag{13}$$

In order to find the correction term in (13), we have computed $N_d t^2/L$ as shown in Fig. 9. We have obtained a straight line from which we get

$$\rho = \frac{0.322}{t} + \frac{0.334}{t^2} + \cdots. \tag{14}$$

This last result is the same for L even and odd. Notice that the correction term in (14) is not given by the scaling function (5).

We have also computed the fluctuation of the density as a function of time and got

$$\frac{\langle\rho^2\rangle - \langle\rho\rangle^2}{\langle\rho\rangle^2} \approx \frac{0.237}{t^{1.00}}. \tag{15}$$

We would like to compare our results with known results obtained for diffusion and annihilation reactions ($A+A\to 0$) with Lévy flights [11–15]. In one dimension, for Lévy flights given by Eq. (2), one gets [12]

$$\rho \sim \begin{cases} t^{-1/\sigma} & \text{for } \sigma > 1, \\ \dfrac{\ln t}{t} & \text{for } \sigma = 1, \\ t^{-1} & \text{for } \sigma < 1, \end{cases} \tag{16}$$

the critical dimension being $d_c = \sigma$.

If one compares (16) for $\sigma=1$, as obtained in Sec. III and (14), one notices the absence of the $\ln t$ correction. Such a term, if present, could have been seen in our simulations (one observes that, for large lattices, ρt converges to the value 0.322 from above). Logarithmic corrections can also appear in a conformal field theory if one has Jordan cells [16] but there are no Jordan cells in the Hamiltonian (A2) given in Appendix A [17]. We believe that the discrepancy between the results of our model and those obtained for the reaction $A+A\rightarrow 0$ comes from the fact that the two models have little in common.

V. CONCLUSIONS

We have presented an extension of the raise and peel model taking into account defects. The main property of this model is that conformal invariance is preserved. The model mimics a system in which particles move in a disordered unquenched medium doing Lévy flights and changing the medium during the flights. Upon contact the defects annihilate. The properties of the system are simple and could be guessed on simple grounds based on conformal invariance. Conformal field theory enters in the description of the scaling function $N_d=f(t/L)$ (N_d is the number of defects, L the size of the system, and t the time).

The original raise and peel model [2] (this is the present model with the defects absent) depends on a parameter w which is the ratio of the desorption and adsorption rates. If $w=1$, one has conformal invariance and the dynamic critical exponent $z=1$. If one takes $0<w<1$, in the disordered medium one has fewer clusters and z varies continuously in the interval $0<z<1$. One can add defects to the model and repeat the exercise done in this paper for all values of w. In this case one expects to find defects making Lévy flights with a probability distribution function

$$P(s)\sim\frac{1}{s^{1+z}}. \tag{17}$$

ACKNOWLEDGMENTS

We thank H. Hinrichsen for a careful reading of the manuscript. This work has been partially supported by the Brazilian agencies FAPESP and CNPq, and by the Australian Research Council.

APPENDIX A: THE CONNECTION BETWEEN TEMPERLEY-LIEB STOCHASTIC PROCESSES AND THE RAISE AND PEEL MODEL

We briefly review this connection; for details see [4,18] and [5].

Consider the Temperley-Lieb semigroup algebra G defined by $L-1$ generators e_j ($j=1,\ldots,L-1$) and the relations

$$e_j^2=e_j,\quad e_je_{j\pm1}e_j=e_j,$$

$$e_je_k=e_ke_j\quad\text{for } |j-k|>1, \tag{A1}$$

and the Hamiltonian

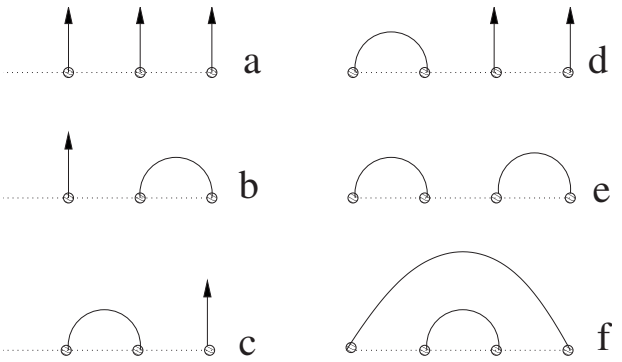

FIG. 10. Six links-defects diagrams for $L=4$. The diagrams (a)–(f) correspond to the RSOS (a)–(f) configurations of Fig. 2.

$$H=\sum_{j=1}^{L-1}(1-e_j). \tag{A2}$$

In the basis $\{w_c\}$ of the words of G (the regular representation of G), H is a matrix satisfying $H_{a,b}\leq 0$ for $a\neq b$ and $\Sigma_b H_{a,b}=0$. Such a matrix is an intensity matrix and defines a Markov process in continuum time given by the master equation

$$\frac{d}{dt}P_a(t)=-\sum_b H_{a,b}P_b(t), \tag{A3}$$

where $P_a(t)$ is the (unnormalized) probability to find the system in the state $|a\rangle$ at time t, and the rate for the transition $|b\rangle\rightarrow|a\rangle$ is given by $-H_{a,b}$, which is non-negative. The Hamiltonian (A2) has an eigenvalue equal to zero. The corresponding left eigenvector $\langle 0|$ is trivial; the right eigenvector $|0\rangle$ gives the probabilities in the stationary state:

$$\langle 0|H=0,\quad \langle 0|=\sum_a\langle a|,$$

$$H|0\rangle=0,\quad |0\rangle=\sum_a P_a|a\rangle,\quad P_a=\lim_{t\rightarrow\infty}P_a(t). \tag{A4}$$

H defined by (A2) gives a Markov process not only if it acts in the vector space of the regular representation but also if it acts in the vector space of a left ideal I because the generators e_j map the left ideal into the left ideal:

$$e_jI=I. \tag{A5}$$

An easy way to define the left ideal in which we are interested and the action of the generators on this ideal is to use the language of graphs.

The generators e_j can be pictorially represented by

e_j =

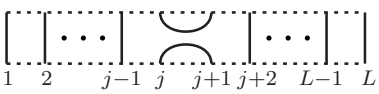

(A6)

The elements of the ideal can be represented by links-defects diagrams. They can be obtained in the following way (see Fig. 10 for $L=4$). Take L sites. If a site is not connected to another one, draw a vertical arrow. Two sites can be connected by a link. The links do not cross each other and the

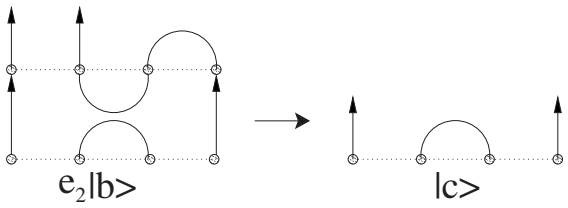

FIG. 11. Action of e_2 on the diagram b of Fig. 10.

arrows cannot cross the links. For a given L the number of diagrams with m defects is

$$C_{L,m} = \binom{L}{\left[\frac{L-m+1}{2}\right]} - \binom{L}{\left[\frac{L-m-1}{2}\right]} \tag{A7}$$

and the total number of diagrams is

$$\sum_{s=0}^{L/2} C_{L,2s+(L \bmod 2)} = \binom{L}{\left[\frac{L}{2}\right]}, \tag{A8}$$

where $[x]$ is the integer part of x.

The action of e_j on a links-defects diagram is given by placing the graph of e_j underneath the first diagram, removing the closed loops and the intermediate dashed line. Next one contracts the links in the composite picture. In Fig. 11 we show the action of e_2 on the diagram of Fig. 10(b).

The action of the Hamiltonian (A2) in the vector space given in Fig. 10 is

$$H = \begin{pmatrix} 3 & 0 & 0 & 0 & 0 & 0 \\ -1 & 2 & -1 & 0 & 0 & 0 \\ -1 & -1 & 2 & -1 & 0 & 0 \\ -1 & 0 & -1 & 2 & 0 & 0 \\ 0 & -1 & 0 & -1 & 1 & -2 \\ 0 & 0 & 0 & 0 & -1 & 2 \end{pmatrix}. \tag{A9}$$

Notice that H has a block triangular form. The stationary state $|0\rangle = 2|e\rangle + |f\rangle$ contains only the two states without arrows (defects) $|e\rangle$ and $|f\rangle$. The various transition rates can be obtained from the matrix elements of H.

In Appendix B we are going to use a 2^L-dimensional representation of the $L-1$ generators e_j and of the Hamiltonian (A2). In this representation, the Hamiltonian describes a spin-1/2 quantum chain. Where can we find the eigenvalues of the left ideal [their number is given by (A8)], among the 2^L eigenvalues of the quantum chain? We are going to give an "almost correct" explanation. We take again the case $L=4$ as an example. If on each of the four sites of the chain one takes a spin-1/2 representation of sl(2), one finds the representation with spin 0 (two times), spin 1 (three times), and spin 2 (one time). If for each representation containing $2s+1$ states (s is the spin) one takes only the highest-weight states, one gets precisely six states (the vertical arrows in Fig. 10 corresponding to up spins).

We give now the correspondence between the links-defects diagrams and the RSOS configurations considered in Sec. II. For a links-defects diagram with L sites ($i=1,2,\ldots,L$), take the dual lattice with $L+1$ sites (on each bond between the sites i and $i+1$ of the links-defects diagram you take the site i on the dual lattice). On the dual lattice we have the sites j ($j=0,1,\ldots,L$). An arrow (defect) on the site i on the links-defects diagram stays unchanged on the dual lattice (it is on the bonds of the dual lattice). For the links, one proceeds as follows. One takes a site on the dual lattice and a vertical line on this site. One counts how many links are cut by the vertical line and one takes a vertex with a height h equal to the number of intersections. Figures 2 and 10 illustrate the rules.

APPENDIX B: THE FINITE-SIZE SCALING LIMIT OF THE HAMILTONIAN EIGENSPECTRUM: RESULTS FROM CONFORMAL FIELD THEORY

We are going to give a brief description of the time evolution operator of the stochastic model described in Sec. II. Firstly we consider the spin-$\frac{1}{2}$ quantum chain defined by the Hamiltonian

$$H = \sum_{i=1}^{L-1} (1 - e_i), \tag{B1}$$

where

$$e_i = \frac{1}{2}\left(\sigma_i^x \sigma_{i+1}^x + \sigma_i^y \sigma_{i+1}^y - \frac{1}{2}\sigma_i^z \sigma_{i+1}^z + i\frac{\sqrt{3}}{2}(\sigma_i^z - \sigma_{i+1}^z)\right), \tag{B2}$$

and $\sigma^x, \sigma^y, \sigma^z$ are Pauli matrices. The Hamiltonian (B1) commutes with

$$S^z = \frac{1}{2}\sum_{i=1}^{L} \sigma_i^z. \tag{B3}$$

In the continuous time limit, the evolution of the system is given by a Hamiltonian H^e which corresponds to the subspace of highest weight $U_q(\mathrm{Sl}(2))$ representations ($q = \exp i\pi/3$) [19]. There are $\binom{L}{[L/2]}$ states in these two sectors ($[x]$ is the integer part of x). If we denote by E_r ($r=0,1,\ldots$) the energy levels in nondecreasing order, $E_0=0 < E_1 \leq E_2 \leq \cdots$, the partition function giving the finite-size scaling limit of the spectrum of H^e is defined as follows:

$$Z(q) = \lim_{L\to\infty} Z_L(q) = \lim_{L\to\infty} \sum_n q^{LE_n/\pi v_s}, \tag{B4}$$

where $v_s = 3\sqrt{3}/2$. One can show [20] that $Z(q)$ has the expression

$$Z(q) = \sum_s \zeta_s(q). \tag{B5}$$

Here s is the spin, taking the values $s=0,1,2,\ldots$ for L even and $s=\frac{1}{2},\frac{3}{2},\frac{5}{2}$ for L odd, and

$$\zeta_s(q) = q^{\Delta_s}(1-q^{2s+1})\prod_{n=1}^{\infty}(1-q^n)^{-1}, \tag{B6}$$

where

$$\Delta_s = \frac{s(2s-1)}{3}. \tag{B7}$$

Moreover, for large lattice sizes, the energies are [see (B4) and (B6)]

$$E = \frac{3\pi\sqrt{3}}{2L}(\Delta_s + k), \tag{B8}$$

where k is an integer.

The Hamiltonian H^e has a block diagonal form. The states with no defects (L even) and those with one defect (L odd) are in one block. This is the $s=0$ $\left(s=\frac{1}{2}\right)$ part of (B5). The states with defects (L even) and more than one defect (L odd) correspond to higher spins. In Sec. III we found that the following values of Δ_s were useful:

$$\Delta_1 = \frac{1}{3}, \quad \Delta_2 = 2 \quad (L \text{ even}),$$

$$\Delta_{3/2} = 1, \quad \Delta_{5/2} = \frac{10}{3} \quad (L \text{ odd}). \tag{B9}$$

[1] J. de Gier, B. Nienhuis, P. Pearce, and V. Rittenberg, J. Stat. Phys. **114**, 1 (2004).
[2] F. C. Alcaraz, E. Levine, and V. Rittenberg, J. Stat. Mech.: Theory Exp. (2006) P08003.
[3] J. de Gier and P. Pyatov, J. Stat. Mech.: Theory Exp. (2004) P0403002.
[4] P. Pyatov, J. Stat. Mech.: Theory Exp. (2004) P09003.
[5] F. C. Alcaraz, P. Pyatov, and V. Rittenberg (unpublished).
[6] M. T. Batchelor, J. de Gier, and B. Nienhuis, J. Phys. A **34**, L265 (2001).
[7] J-P. Bouchaud and A. Georges, Phys. Rep. **195**, 127 (1990).
[8] H. C. Fogedby, Phys. Rev. Lett. **73**, 2517 (1994).
[9] E. R. Weeks, T. H. Solomon, J. S. Urbach, and H. L. Swinney, in *Lévy Flights and Related Topics in Physics*, edited by M. F. Schlessinger, G. M. Zaslavsky, and U. Frish (Springer-Verlag, Heidelberg, 1995).
[10] S. Jespersen, R. Metzler, and H. C. Fogedby, Phys. Rev. E **59**, 2736 (1999).
[11] E. V. Albano, J. Phys. A **24**, 3351 (1991).
[12] H. Hinrichsen and M. Howard, Eur. Phys. J. B **7**, 635 (1999).
[13] D. Vernon and M. Howard, Phys. Rev. E **63**, 041116 (2001).
[14] D. C. Vernon, Phys. Rev. E **68**, 041103 (2003).
[15] U. Tauber, M. Howard, and B. Vollmayr-Lee, J. Phys. A **38**, R79 (2005).
[16] M. P Gaberdiel, Int. J. Mod. Phys. A **18**, 4593 (2003).
[17] Paul Pearce (private communication).
[18] P. P. Pearce, V. Rittenberg, J. de Gier, and B. Nienhuis, J. Phys. A **35**, L661 (2002).
[19] V. Pasquier and H. Saleur, Nucl. Phys. B **330**, 523 (1990).
[20] H. Saleur and M. Bauer, Nucl. Phys. B **320**, 591 (1989).